

Preservation of orientation of fusion-evaporation reaction residues recoiling into vacuum in a level mixing spectroscopy experiment

K. Vyvey, G. Neyens, N. Coulier, R. Coussement, G. Georgiev, S. Ternier, and S. Teughels
Instituut voor Kern- en stralingsfysica, University of Leuven, Celestijnenlaan 200 D, B-3001 Leuven, Belgium

A. Lépine-Szily
Institute of Physics, University of São Paulo, 66318, 05389-970 São Paulo, Brazil

D. L. Balabanski
Faculty of Physics, St. Kliment Ohridsky University of Sofia, BG-1164 Sofia, Bulgaria
 (Received 3 April 2000; published 22 August 2000)

The interaction between the nuclear spin \vec{I} and the atomic spin \vec{J} of the not fully stripped nuclei, which are recoiling after a nuclear reaction, reduces the nuclear orientation during their flight through vacuum. In this paper we report on how the orientation is restored by applying a magnetic field in the direction of the initial orientation axis. This implies that the level mixing spectroscopy technique (LEMS), used to measure nuclear quadrupole moments of high-spin isomers, can be applied for nuclei which have traveled through a vacuum before being implanted in a suitable host. Such a recoil-shadow configuration, where target and host are separated from each other and the detectors are shielded from the target, improves the detection efficiency in a LEMS setup. This increases the possibilities for application of the LEMS method. We have developed a formalism that describes the loss of orientation due to the $\vec{I} \cdot \vec{J}$ interaction and its influence on a LEMS measurement performed in a recoil-shadow geometry. The formalism is used to describe experimental data for the $^{69m}\text{Ge}[I^\pi=9/2^+, \tau=4.05(7)\mu\text{s}, \mu=-1.0011(32)\text{ nm}]$ isomers recoiling out of a ^{56}Fe target into a Ni and a Pt host.

PACS number(s): 23.20.En, 21.10.Ky, 27.50.+e, 31.30.Gs

I. INTRODUCTION

Measured quadrupole moments provide direct information on the deformation of the nucleus and therefore provide a stringent test for nuclear calculations. Especially for nuclei having extreme characteristics, i.e., nuclei with high isospin or high spin, it is interesting to test experimentally the validity of these models. The family of level mixing techniques has proven to be a very powerful tool for measuring quadrupole moments of a wide variety of nuclei. While recently the level mixing resonance (LMR) technique [1] has been extended for quadrupole moment studies of β -decaying nuclei with high isospin [2–5], its variant level mixing spectroscopy (LEMS) is suitable for measuring quadrupole moments of γ -decaying nuclei with high spin [6–9].

Similar to all level mixing techniques, LEMS is based on the change of the anisotropy of the emitted radiation as a function of the magnetic field strength due to a combined magnetic dipole and electric quadrupole interaction. The electric field gradient (EFG) is provided by the internal crystalline fields after in-beam implantation of the reaction residues in a suitable host. The magnetic field is provided by a superconducting magnet. In this paper we will add a third interaction. This interaction is due to the coupling of the nuclear spin \vec{I} and the atomic spin \vec{J} during the flight through vacuum of the isomers of interest. This extension allows the use of the recoil-shadow configuration, i.e., separating target and host and shielding the detectors from the target, to improve the peak to background ratio in a LEMS experiment. This increases the applicability of the LEMS technique. At

this point, fusion-evaporation reactions are used to produce the isomers of interest. The use of the recoil-shadow configuration will reduce the prompt background radiation coming from the target to allow the measurement of weakly populated isomers. A complicating factor for the application of the recoil-shadow technique is that in most of the cases (usually for the energies of the fusion-evaporation reactions of interest) the recoiling nuclei are not fully stripped. Thus there is a loss in the nuclear spin orientation due to the interaction between the randomly oriented atomic spin \vec{J} and the nuclear spin \vec{I} during the flight through the vacuum. As the orientation will be restored by applying a sufficiently large magnetic field in the direction of the initial orientation axis, a change in the anisotropy as a function of the magnetic field strength will be measured. This means that the influence of the $\vec{I} \cdot \vec{J}$ interaction on the anisotropy of the radiation, as a function of the magnetic field strength, should be investigated in order to ensure a correct quadrupole moment determination.

Section II contains a theoretical study of the influence of the combined $\vec{I} \cdot \vec{J}$ + magnetic dipole interaction and the combined $\vec{I} \cdot \vec{J}$ + magnetic dipole + electric quadrupole interaction on the anisotropy of the radiation. Experimental results on the known $^{69}\text{Ge}[I^\pi=9/2^+, \tau=4.05(7)\mu\text{s}, \mu=-1.0011(32)\text{ nm}, Q=1.0(2)e\text{ b} [10]]$ isomers recoiling in a Ni host and a Pt host, respectively, will be presented in Sec. III. In addition to testing experimentally the improvement of the peak to background ratio in a recoil-shadow geometry and the applicability of the LEMS technique in

combination with the recoil-shadow configuration, these experiments also reveal information on the magnetic hyperfine field, caused by the atomic electrons at the position of the nucleus B_{hf} , and the atomic structure of the ^{69}Ge atoms recoiling out of an Fe target with an average velocity of $v/c = 1.7\%$, which will be discussed elsewhere [11].

II. THE INFLUENCE OF THE $\vec{I}\cdot\vec{J}$ INTERACTION ON THE LEMS TECHNIQUE

The principles of the LEMS technique have been extensively treated in Ref. [6], while the formalism of the $\vec{I}\cdot\vec{J}$ interaction is discussed in Refs. [12–15]. Here we will briefly review the main features relevant for including the $\vec{I}\cdot\vec{J}$ interaction in the LEMS formalism.

A. The LEMS technique

In the LEMS technique the electric quadrupole interaction is studied by submitting the isomers of interest to a combined electric quadrupole and magnetic dipole interaction which are misaligned with an angle β . In the axis system with the Z-axis parallel to the magnetic field direction (lab system), the Hamiltonian of the magnetic interaction can be written as

$$\mathcal{H}_B = -\omega_B I_Z, \quad (1)$$

where $\omega_B = g\mu_N B_0/\hbar$ is the magnetic interaction frequency. For an axially symmetric electric field gradient, the Hamiltonian of the quadrupole interaction can be written in the principle axis system (PAS) of the EFG

$$\mathcal{H}_Q = \frac{\omega_Q}{\hbar} (3I_Z^2 - I^2), \quad (2)$$

where $\omega_Q = eQV_{ZZ}/\hbar 4I(2I-1)$ is the electric quadrupole frequency and Q is the spectroscopic quadrupole moment. Transforming \mathcal{H}_Q from the PAS to the lab system and combining both interactions results in the following nonvanishing elements for the LEMS Hamiltonian $\mathcal{H}_{\text{LEMS}}$ [16]:

$$\begin{aligned} \langle m | \mathcal{H}_{\text{LEMS}} | m \rangle &= -\hbar\omega_B m + \hbar\omega_Q \frac{1}{2} (3 \cos^2 \beta - 1) \\ &\quad \times [3m^2 - I(I+1)], \end{aligned} \quad (3)$$

$$\begin{aligned} \langle m | \mathcal{H}_{\text{LEMS}} | m-1 \rangle &= -\frac{3}{2} \hbar\omega_Q \cos \beta \sin \beta (1-2m) \\ &\quad \times \sqrt{(I-m+1)(I+m)}, \end{aligned} \quad (4)$$

$$\langle m | \mathcal{H}_{\text{LEMS}} | m-2 \rangle = \frac{3}{4} \hbar\omega_Q \sin^2 \beta \sqrt{(I+m-1)(I+m)(I-m+1)(I-m+2)}. \quad (5)$$

The nondiagonal elements involve a mixing of the populations of the different m states and are thus responsible for the change of the orientation of the nuclear ensemble. They are only present when the misalignment angle β differs from zero. When polycrystals are used the solution of the time-evolution equation has to be integrated over all possible angles β .

The influence of the perturbation, governed by $\mathcal{H}_{\text{LEMS}}$, on an isomeric state, can be studied by observing the subsequent radiation of this state. The perturbed angular distribution of the radiation is given by [12]

$$W(\theta, \phi, t) = \sqrt{4\pi} \sum_{k,n} \frac{1}{\sqrt{2k+1}} A_k U_k B_k^n(I, t) Y_k^n(\theta, \phi), \quad (6)$$

with A_k being the radiation parameters of the observed transitions, U_k describing the loss of orientation due to nondetected preceding γ rays, $B_k^n(I, t)$ being the orientation tensors at time t and $Y_k^n(\theta, \phi)$ being the spherical harmonics in which θ and ϕ describe the detection directions. The orientation parameters are related to the initial orientation $B_k^{n'}(t=0)$ by [12]

$$B_k^n(I, t) = \sum_{k', n'} G_{kk'}^{nn'}(I, \mathcal{H}_{\text{LEMS}}, t) B_k^{n'}(t=0). \quad (7)$$

The $G_{kk'}^{nn'}(I, \mathcal{H}_{\text{LEMS}}, t)$ are the perturbation factors that contain the influence of the Hamiltonian on the orientation of the levels, as described by the density matrix ρ [12]. The perturbation factor can be calculated explicitly by solving the von Neumann equation $i\hbar(d\rho_{\text{LEMS}}/dt) = [\mathcal{H}_{\text{LEMS}}, \rho]$ from which the time evolution of the density matrix [17] is deduced, using the eigenstates of $\mathcal{H}_{\text{LEMS}}$. Via the direct relationship between the orientation tensors $B_k^n(I, t)$ and the density matrix elements $\langle m'_I | \rho_{\text{LEMS}}(t) | m_I \rangle$ [17], the perturbation factors can be calculated explicitly as

$$\begin{aligned} G_{kk'}^{nn'}(I, \mathcal{H}_{\text{LEMS}}, t) &= \sqrt{2k+1} \sqrt{2k'+1} \sum_{m_I, \mu_I, N, N'} (-1)^{m_I - \mu_I} \\ &\quad \times \begin{pmatrix} I & I & k \\ -m_I & m'_I & n \end{pmatrix} \\ &\quad \times \begin{pmatrix} I & I & k' \\ -\mu_I & \mu'_I & n' \end{pmatrix} e^{-i\omega_{NN'} t} \langle m_I | N \rangle \\ &\quad \times \langle N | \mu_I \rangle \langle m'_I | N' \rangle^* \langle N' | \mu'_I \rangle^*, \end{aligned} \quad (8)$$

with $\omega_{NN'} = (E_N - E_{N'})/\hbar$. E_N and $|N\rangle$ are the eigenvalues and eigenvectors of $\mathcal{H}_{\text{LEMS}}$. Further the LEMS perturbation factor will be noted as

$$G_{kk'}^{nn'}(I, \mathcal{H}_{\text{LEMS}}, t) = \sum_{NN'} (f_{NN'}^{\text{LEMS}})_{kk'} e^{-i\omega_{NN'}^{\text{LEMS}} t}. \quad (9)$$

The $G_{kk'}^{nn'}$ ($n' \neq 0$) terms are 0 because of the axial symmetry of the orientation of the compound nuclei produced in a fusion-evaporation reaction. If the EFG is provided by a polycrystal, only the $G_{kk'}^{00}$ terms need to be taken into account. This is because of the axial symmetry of all interactions with respect to the symmetry axis of the initial orientation.

As LEMS measurements are time-averaged measurements, a time integration, including a $e^{-t/\tau}$ weight to incorporate the nuclear lifetime of the isomer, has to be made

$$G_{kk'}^{nn'}(I, \mathcal{H}_{\text{LEMS}}, \tau) = \frac{\int_0^\infty G_{kk'}^{nn'}(I, \mathcal{H}_{\text{LEMS}}, t) e^{-t/\tau} dt}{\int_0^\infty e^{-t/\tau} dt}. \quad (10)$$

The result for the anisotropy of the γ radiation as a function of the magnetic field is a decoupling curve, which can be explained in a handwaving way as follows. After production and orientation the isomers of interest are caught in a suitable host where they are submitted to a combined electric quadrupole and magnetic dipole interaction. The magnetic field is oriented parallel to the beam axis, i.e., the symmetry axis of the initial orientation. At zero magnetic field only the quadrupole interaction is present and the initial orientation and anisotropy is decreased to the hard-core value. At high magnetic fields (several T), the electric quadrupole interaction is negligible compared to the Larmor precession of the isomeric spins around \vec{B} . As the precession axis coincides with the initial orientation axis, the initial anisotropy is measured. At intermediate fields there is a competition between the quadrupole and the magnetic interaction and a smooth change from the hard-core anisotropy to the initial full anisotropy takes place. This part of the LEMS curve is sensitive to the ratio of the quadrupole interaction frequency $\nu_Q = eQV_{ZZ}/h$ to the magnetic moment μ of the isomer. So, if the magnetic moment is known, the quadrupole interaction frequency can be deduced.

B. The combined magnetic + $\vec{I} \cdot \vec{J}$ interaction

In free atoms the nuclear spin \vec{I} and the atomic spin \vec{J} interact with each other, coupling to a total angular momentum \vec{F} , around which both \vec{I} and \vec{J} precess. This means that during the flight through the vacuum (when the recoiling atoms are free), nonfully stripped nuclei will be submitted to this $\vec{I} \cdot \vec{J}$ -coupling interaction. As the atomic spin is randomly oriented, the net result of the precession is a lowering of the orientation of the nuclear ensemble. The orientation can be

restored by applying a sufficiently high magnetic field parallel to the nuclear orientation axis so that both the atomic and nuclear spins perform a Larmor precession around this magnetic field [12–15]. As the Bohr magneton is about 2000 times larger than the nuclear magneton, the decoupling occurs when $\langle \vec{\mu}_j \cdot \vec{B} \rangle$ is larger than $\langle a \vec{I} \cdot \vec{J} \rangle$. The Hamiltonian of the interaction is given by [12]

$$\mathcal{H}_{IJ} = a \vec{I} \cdot \vec{J} + \vec{\mu}_j \cdot \vec{B} - \vec{\mu}_I \cdot \vec{B}, \quad (11)$$

with $a = \mu_I \langle B_{\text{hf}}(0) \rangle / I J \hbar^2$ being the coupling constant, $\vec{\mu}_I$ the nuclear magnetic moment, $\vec{\mu}_j$ the electronic magnetic moment, and B_{hf} the hyperfine field induced by the atomic electrons. So, if μ_I is known, B_{hf} can be deduced from the value of a and vice versa.

It can be shown that the nuclear density matrix elements of the two-spin system can be written as [18]

$$\langle m_I | \rho_I(t) | m_I' \rangle = \sum_{m_J} \langle m_I m_J | \rho_{IJ}(t) | m_I' m_J \rangle, \quad (12)$$

with ρ_I the density matrix describing the nuclear spin system and ρ_{IJ} the density matrix describing the total ensemble of nuclear and atomic spins. Further note, since the nuclear spin system and the atomic spin system are not coupled at $t=0$ (the moment of the recoil out of the target), the following relationship holds:

$$\begin{aligned} \langle m_I m_J | \rho_{IJ}(t=0) | m_I' m_J' \rangle \\ = \langle m_I | \rho_I(t=0) | m_I' \rangle \langle m_J | \rho_J(t=0) | m_J' \rangle, \end{aligned} \quad (13)$$

with ρ_J the density matrix describing the atomic spin system. Using the relationships (12) and (13), the $\vec{I} \cdot \vec{J}$ perturbation factor can be calculated in a similar way as the LEMS perturbation factor

$$\begin{aligned} G_{kk'}^{00}(I, J, \mathcal{H}_{IJ}, t) &= \frac{\sqrt{2k+1} \sqrt{2k'+1}}{2J+1} \sum_{m_I, m_J, \mu_I, \mu_J, N, N'} \\ &\times (-1)^{m_I - \mu_I} \begin{pmatrix} I & I & k \\ -m_I & m_I & 0 \end{pmatrix} \\ &\times \begin{pmatrix} I & I & k' \\ -\mu_I & \mu_I & 0 \end{pmatrix} e^{-i\omega_{NN'} t} \langle m_I m_J | N \rangle \\ &\times \langle N | \mu_I \mu_J \rangle \langle \mu_I \mu_J | N' \rangle^* \langle N' | m_I m_J \rangle^*, \end{aligned} \quad (14)$$

with $\omega_{NN'} = (E_N - E_{N'})/\hbar$ and E_N and $|N\rangle$ the eigenvalues and eigenvectors of \mathcal{H}_{IJ} . Further the $\vec{I} \cdot \vec{J}$ perturbation factor will be noted as

$$G_{kk'}^{00}(I, J, \mathcal{H}_{IJ}, t) = \sum_{NN'} (f_{NN'}^{IJ})_{kk'} e^{-i\omega_{NN'} t}. \quad (15)$$

Only the $G_{kk'}^{00}$ terms need to be taken into account, since all interactions are axially symmetric with respect to the symmetry axis of the initial orientation.

The main difference with Refs. [14,15] is the way in which the time integration of the perturbation factor is performed. In Refs. [14,15] it is assumed that all nuclei decay in flight. In our formalism we also consider the case when the nuclei survive the flight and decay in a cubic host (cubic to exclude the quadrupole interaction, which, if present, also influences the anisotropy of the radiation, see Secs. II A and II C). During the time interval $[0, T]$, with T the flight time (of order 10 ns for a recoil-distance of 6 cm), the $\vec{I} \cdot \vec{J}$ interaction will perturb the orientation. Once the nuclei reach the host the orientation is kept, since the $\vec{I} \cdot \vec{J}$ is only active when the atom is free (apart from some exceptional cases where the $\vec{I} \cdot \vec{J}$ interaction is also active in insulators [12,19]). In the time integration of the $\vec{I} \cdot \vec{J}$ perturbation factor, not only a weight $e^{-t/\tau}$ to incorporate the lifetime is taken into account, but also a Gaussian weight over the flight time T : $e^{-(T-T_0)^2/\sigma_T^2}$, with

$$T_0 = \sqrt{\frac{m}{2}} \frac{1}{\sqrt{E_0}} d$$

the average flight time and

$$\sigma_T = \left| \sqrt{\frac{m}{2}} \frac{1}{\sqrt{E_0 - \sigma_E}} d - T_0 \right|$$

the standard deviation. Here d is the recoil distance on which the flight time T_0 and the standard deviation σ_T depend linearly. E_0 is the average energy with which the nuclei leave the target, i.e., the recoil energy minus the loss of energy due to the travel of the nucleus through the target. σ_E is the spread in energy with which the atoms leave the target. This spread in energy, and as a consequence the spread in flight time, is mainly caused due to the fact that the nuclei are produced throughout the whole target thickness and follow different trajectories before leaving the target, resulting in different energy losses, which can, e.g., be demonstrated by TRIM [20] calculations.

The following expression for the time integrated $\vec{I} \cdot \vec{J}$ perturbation factor is obtained:

$$G_{kk'}^{00}(I, J, \mathcal{H}_{IJ}, \tau, T_0) = \frac{\int_0^\infty e^{-(T-T_0)^2/\sigma_T^2} \left(\int_0^T e^{-t/\tau} G_{kk'}^{00}(I, J, \mathcal{H}_{IJ}, t) + G_{kk'}^{00}(I, J, \mathcal{H}_{IJ}, T) \int_T^\infty e^{-t/\tau} \right) dt dT}{\int_0^\infty e^{-(T-T_0)^2/\sigma_T^2} \int_0^\infty e^{-t/\tau} dt dT}. \quad (16)$$

The integrals can be calculated in an analytical way, resulting in

$$\begin{aligned} G_{kk'}^{00}(I, J, \mathcal{H}_{IJ}, \tau, T_0) = & \sum_{NN'} (f_{NN'}^{IJ})_{kk'} \left\{ \frac{1}{1 + (\omega_{NN'}^{IJ} \tau)^2} \right. \\ & + \frac{e^{-T_0/\tau - (\sigma_T^2/4\tau^2)[(\omega_{NN'}^{IJ} \tau)^2 - 1]}}{1 + (\omega_{NN'}^{IJ} \tau)^2} \\ & \times \left[-\cos\left(-\omega_{NN'}^{IJ} T_0 + \frac{\sigma_T^2 \omega_{NN'}^{IJ}}{2\tau}\right) \right. \\ & \left. \left. - \omega_{NN'}^{IJ} \tau \sin\left(-\omega_{NN'}^{IJ} T_0 + \frac{\sigma_T^2 \omega_{NN'}^{IJ}}{2\tau}\right) \right] \right. \\ & \left. + e^{-T_0/\tau - (\sigma_T^2/4\tau^2)[(\omega_{NN'}^{IJ} \tau)^2 - 1]} \right. \\ & \left. \times \left[\cos\left(-\omega_{NN'}^{IJ} T_0 + \frac{\sigma_T^2 \omega_{NN'}^{IJ}}{2\tau}\right) \right] \right\}. \quad (17) \end{aligned}$$

Usually the last two terms are negligible: for small $\omega_{NN'}^{IJ} \tau$ they cancel each other, for large $\omega_{NN'}^{IJ} \tau$ the exponentials go to 0. This means that in most of the cases the expression reduces to the $1/[1 + (\omega_{NN'}^{IJ} \tau)^2]$ term, i.e., the term which is obtained by assuming all nuclei decay in flight, which is the result considered in Refs. [13–15]. However the $G_{kk'}^{00}(I, J, \mathcal{H}_{IJ}, \tau, T_0)$ perturbation factors should go to 1 and the $G_{kk'}^{00}(I, J, \mathcal{H}_{IJ}, \tau, T_0)$, $k \neq k'$ perturbation factors to 0 when the interaction time approaches 0. The interaction time is equal to the lifetime of the nucleus or the flight time, depending on which of them is the shortest. It is clear from expression (17) that for a zero flight time (both T_0 and σ_T going to 0) this condition is only fulfilled when the last two terms are present. So they are necessary in the case when a short flight time reduces the interaction time too much to reach the hard core value for the anisotropy.

Note that in reality not the flight time distribution, but the energy distribution is a Gaussian, resulting in a $(md^2/T^3) e^{-\sigma_T'^4(1/T^2 - 1/T_0^2)^2} dT$ distribution function for the flight time T . Here σ_T' is defined as $\sqrt{m/2}(1/\sqrt{\sigma_E})d$. The latter distribution function results in a summation of integrals which have to be calculated in a numerical way. We prefer to mention the Gaussian approach in this paper, because its

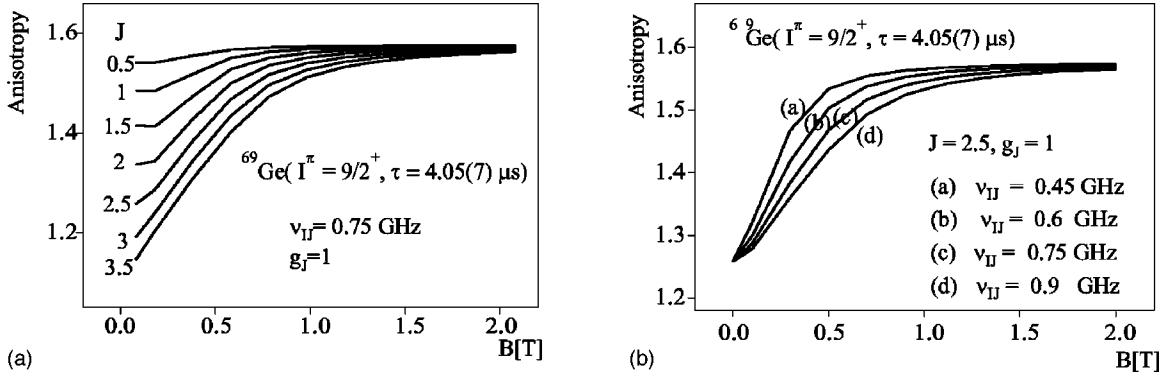


FIG. 1. Simulations of the change in the anisotropy as a function of the magnetic field due to the combined $\vec{I} \cdot \vec{J}$ + magnetic dipole interaction for the $^{69}\text{Ge}(I^\pi = 9/2^+, \tau = 4 \mu\text{s}, \mu = -1.0011(32) \text{ nm})$ isomer. In (a) the atomic spin J has been varied, in (b) the $\vec{I} \cdot \vec{J}$ interaction frequency $\nu_{IJ} = (\hbar/2\pi)a$ has been varied.

analytical solution has a direct physical interpretation. Only when the flight time is too short to reach the hardcore value for the anisotropy, the results obtained by using the Gaussian approximation for T differ up to 15% from the correct ones. In all other cases the difference is negligible. In addition it is straightforward that the calculation time will be a lot longer when numerical calculations for the integrals are needed.

Simulations of the anisotropy as a function of the magnetic field for the combined magnetic + $\vec{I} \cdot \vec{J}$ interaction are shown in Fig. 1 for the $^{69}\text{Ge}[I^\pi = 9/2^+, \tau = 4.05(7) \mu\text{s}, \mu = -1.0011(32) \text{ nm}]$ isomer. Figure 1(b) shows that the $\vec{I} \cdot \vec{J}$ interaction frequency $\nu_{IJ} = (\hbar/2\pi)a$ influences the decoupling value of the curve. The larger ν_{IJ} , and thus the interaction between the atomic electrons and the nucleus, the larger the decoupling field. This can also be understood from the condition $\langle \vec{\mu}_j \cdot \vec{B} \rangle > \langle a \vec{I} \cdot \vec{J} \rangle$. Figure 1(a) shows that the amplitude of the curve depends on the atomic spin J , more precisely on the ratio of the atomic spin J to the nuclear spin

I . Intuitively it is clear that a large atomic spin J compared to the nuclear spin I will disturb the nuclear orientation a lot more, than a smaller one [13].

C. The LEMS formalism including the $\vec{I} \cdot \vec{J}$ interaction

If there is a recoil-distance between target and host and an EFG is present in the host, consecutively the combined $\vec{I} \cdot \vec{J}$ + magnetic dipole interaction (during recoil) and the combined electric quadrupole + magnetic dipole interaction (after implantation) take place. The change of the orientation during the time interval $[0, T]$ is taken into account by the $\vec{I} \cdot \vec{J}$ perturbation factor $G_{kk'}^{00}(I, J, \mathcal{H}_{IJ}, t)$ and the change in the time interval $[T, \infty]$ by the LEMS perturbation factor $G_{kk'}^{nn'}(I, \mathcal{H}_{LEMS}, t)$. The time integration, again including a weight $e^{-t/\tau}$ to incorporate the nuclear lifetime and a Gaussian weight for the flight time, results in

$$G_{kk'}^{00}(I, J, \mathcal{H}_{IJ} + \mathcal{H}_{LEMS}, \tau, T_0) = \frac{\int_0^\infty e^{-(T-T_0)^2/\sigma_T^2} \int_0^T e^{-t/\tau} G_{kk'}^{00}(I, J, \mathcal{H}_{IJ}, t) dt dT}{\int_0^\infty e^{-(T-T_0)^2/\sigma_T^2} dT \int_0^\infty e^{-t/\tau} dt} + \frac{\sum_I \int_0^\infty e^{-(T-T_0)^2/\sigma_T^2} G_{kl}^{00}(I, J, \mathcal{H}_{IJ}, T) \int_T^\infty e^{-t/\tau} G_{lk'}^{00}(I, \mathcal{H}_{LEMS}, t) dt dT}{\int_0^\infty e^{-(T-T_0)^2/\sigma_T^2} dT \int_0^\infty e^{-t/\tau} dt}. \quad (18)$$

Again an analytical solution is obtained:

$$\begin{aligned}
G_{kk'}^{00}(I, J, \mathcal{H}_{IJ} + \mathcal{H}_{\text{LEMS}}, \tau, T_0) = & \sum_{NN'} (f_{NN'}^{IJ})_{kk'} \frac{1}{1 + (\omega_{NN'}^{IJ}, \tau)^2} \left\{ 1 + e^{-T_0/\tau - \sigma^2/4\tau^2 [(\omega_{NN'}^{IJ}, \tau)^2 - 1]} \left[-\cos\left(-\omega_{NN'}^{IJ} T_0 + \frac{\sigma^2 \omega_{NN'}^{IJ}}{2\tau}\right) \right. \right. \\
& \left. \left. - \omega_{NN'}^{IJ} \tau \sin\left(-\omega_{NN'}^{IJ} T_0 + \frac{\sigma^2 \omega_{NN'}^{IJ}}{2\tau}\right) \right] \right\} \\
& + \sum_I \sum_{NN'} \sum_{MM'} (f_{NN'}^{IJ})_{kl} (f_{MM'}^{\text{LEMS}})_{lk'} \frac{1}{1 + (\omega_{MM'}^{\text{LEMS}}, \tau)^2} e^{-T_0/\tau - \sigma^2/4\tau^2 [(\omega_{NN'}^{IJ} + \omega_{MM'}^{\text{LEMS}}) \tau]^2 - 1} \\
& \times \left[\cos\left(-(\omega_{NN'}^{IJ} + \omega_{MM'}^{\text{LEMS}}) T_0 + \frac{\sigma^2 (\omega_{NN'}^{IJ} + \omega_{MM'}^{\text{LEMS}})}{2\tau}\right) + \omega_{MM'}^{\text{LEMS}} \tau \sin\left(-(\omega_{NN'}^{IJ} + \omega_{MM'}^{\text{LEMS}}) T_0 \right. \right. \\
& \left. \left. + \frac{\sigma^2 (\omega_{NN'}^{IJ} + \omega_{MM'}^{\text{LEMS}})}{2\tau}\right) \right]. \tag{19}
\end{aligned}$$

We restrict ourselves to the $G_{kk'}^{00}$ terms, because in a LEMS experiment usually a polycrystal is providing the EFG [6]. In this case all interactions are axially symmetric with respect to the initial orientation axis. If a single crystal is used, the $G_{kk'}^{n0}$ ($n \neq 0$) terms need to be considered [6].

If no quadrupole interaction takes place, the expression for $G_{kk'}^{00}(I, J, \mathcal{H}_{IJ} + \mathcal{H}_{\text{LEMS}}, \tau, T_0)$ reduces to the $G_{kk'}^{00}(I, J, \mathcal{H}_{IJ}, \tau, T_0)$ perturbation factor. This is also the case when all nuclei decay in flight ($T_0 > \tau$). When no recoil distance is present ($T_0 = \sigma_T = 0$) the expression reduces to the $G_{kk'}^{00}(I, \mathcal{H}_{\text{LEMS}}, \tau)$ perturbation factor. If no $\vec{I} \cdot \vec{J}$ interaction takes place during the flight through the vacuum, e.g., because the recoiling ions are fully stripped or are in an atomic noble-gas-like configuration [21–23], the pure LEMS perturbation factor is not immediately obtained. If part of the nuclei does not reach the host (T_0 comparable to or smaller than the nuclear lifetime τ), the LEMS amplitude will be reduced. Only when all nuclei reach the host ($\tau \gg T_0$), the hardcore value of the anisotropy due to the combined electric quadrupole + magnetic dipole interaction will be reached.

Figure 2 shows some simulations of a LEMS curve, a combined magnetic dipole + $\vec{I} \cdot \vec{J}$ interaction, and a combined $\vec{I} \cdot \vec{J}$ interaction + magnetic dipole + electric quadrupole interaction, respectively, for the $^{69m}\text{Ge}(I^\pi = 9/2^+)$ isomer, leaving the target with an energy and an energy spread typical for a fusion-evaporation reaction: $E_0 = 9$ MeV and $\sigma_E = 5$ MeV. When the atomic spin J is small compared to the nuclear spin I , resulting in an amplitude of the $\vec{I} \cdot \vec{J}$ curve which is smaller than the amplitude of the LEMS curve, and the magnetic field necessary to decouple the $\vec{I} \cdot \vec{J}$ interaction is smaller than the magnetic field necessary to decouple the quadrupole interaction, the influence of the $\vec{I} \cdot \vec{J}$ interaction on the LEMS curve is negligible [Fig. 2(a)]. These two conditions are usually fulfilled: the LEMS technique is especially designed to measure quadrupole moments of high-spin isomers (up to $I = 40$) and even for a large hyperfine field of 10^3 T, a magnetic field of only 0.8 T is sufficient to decouple

the $\vec{I} \cdot \vec{J}$ interaction (Sec. III B). To decouple the quadrupole interaction very often magnetic fields of several T are necessary, depending on the nuclear deformation and the magnetic moment of the isomer of interest. Only in the case of a reduced LEMS amplitude, e.g., when the nuclei are implanted in a cubic lattice and only part of them interact with a defect-associated EFG [Fig. 2(b)], or in the exceptional case that the atomic spin J is comparable to the nuclear spin I and a large hyperfine field is present ($I = 9/2$, $J = 7/2$, and $\nu_{IJ} = 1.25$ GHz) [Fig. 2(c)], the $\vec{I} \cdot \vec{J}$ interaction has an important influence on the LEMS curve, as is demonstrated in Figs. 2(b) and 2(c).

III. EXPERIMENTAL RESULTS

A. The improvement of the peak to background ratio in a recoil-shadow configuration

Since LEMS is a decoupling technique, large homogeneous fields (order of several T) are needed at the target position. Therefore the number of holes in the split-coil superconducting magnet and thus the number of detector positions is limited, so that the usual means to clean the spectra, e.g., measuring coincidence spectra, cannot be applied due to the low counting rates. Also the use of anti-Compton shields is not straightforward for the simple reason that the phototubes do not work in the stray magnetic field, which can go as high as 1 T. Substantial technical development would be needed for this case. At this point, the only way to reduce the prompt background radiation is by pulsing the beam and measuring during the beam-off period only. However, this method is most powerful when one has beam pulsing with a period of the order of the lifetime of the isomer of interest. For short lifetimes (lower than 300 ns) the external high voltages needed to pulse the cyclotron beam cannot be switched on and off fast enough with the present technology. This problem is solved by using the HF signal of the cyclotron itself, but the technique loses much of its efficiency this way, because the typical time between the beam bursts is only 50 to 80 ns in this case, while the time resolution of a

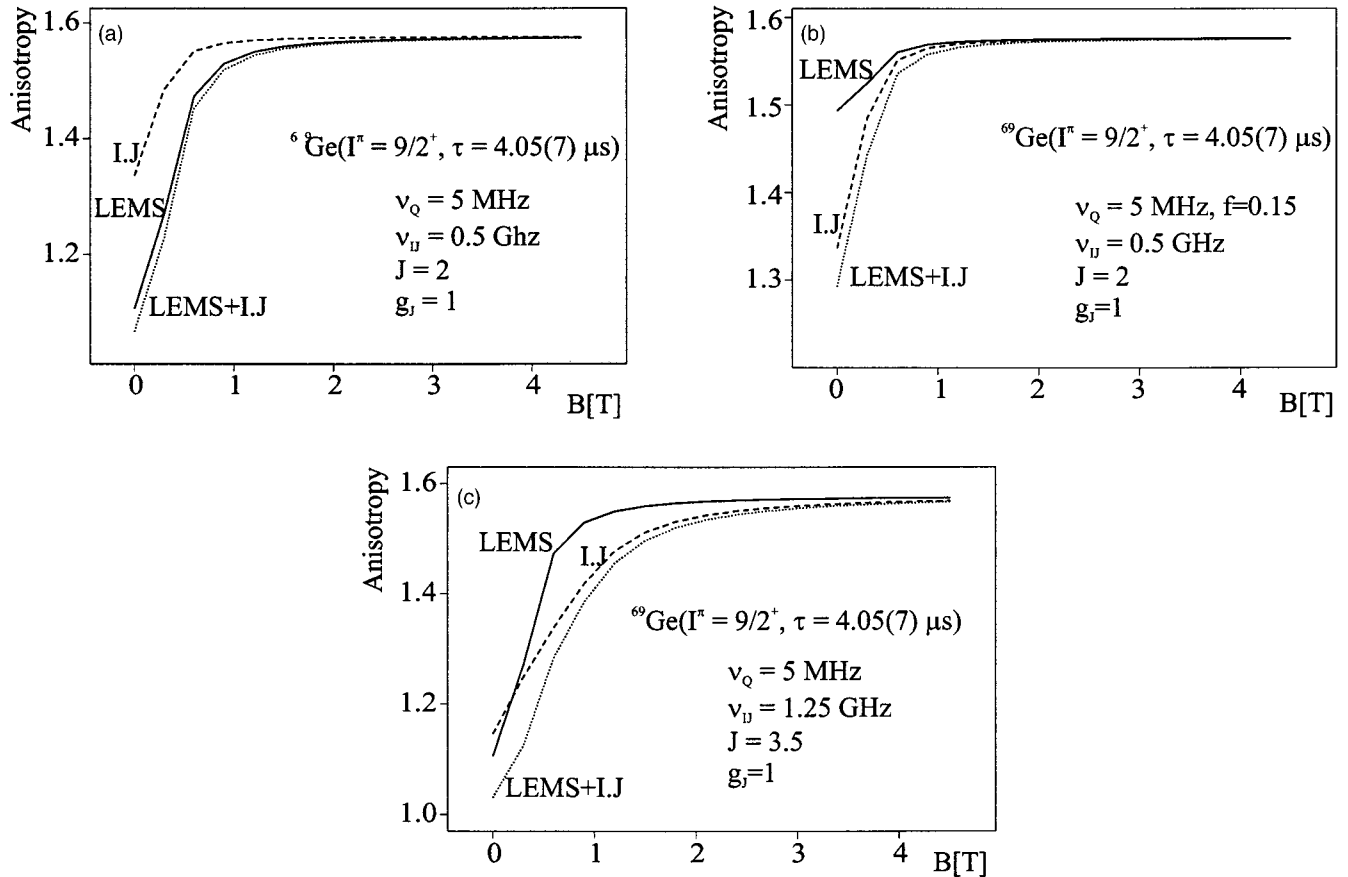


FIG. 2. Simulations demonstrating the influence of the $\vec{I} \cdot \vec{J}$ interaction on a LEMS curve for the $^{69m}\text{Ge}[I^\pi = 9/2^+, \mu = -1.0011(32) \text{ nm}, \tau = 4.05(7) \mu\text{s}]$ isomer. The solid line represents the LEMS curve, the dashed line the $\vec{I} \cdot \vec{J}$ decoupling curve and the dotted line the combined LEMS + $\vec{I} \cdot \vec{J}$ decoupling curve. In (a) typical values for the quadrupole interaction frequency ν_Q , the $\vec{I} \cdot \vec{J}$ interaction frequency ν_{IJ} and the atomic spin J have been taken. The influence of the $\vec{I} \cdot \vec{J}$ interaction on the LEMS curve is negligible. In (b) the $\vec{I} \cdot \vec{J}$ interaction frequency ν_{IJ} and the atomic spin J take typical values, but the amplitude of the LEMS curve is reduced, because only 15% of the nuclei are interacting with an EFG. Physically this can be a case when the Ge atoms are implanted in a cubic lattice and a part of them interact with a defect-associated EFG. In (c) the $\vec{I} \cdot \vec{J}$ interaction has been taken to be exceptionally strong compared to the quadrupole interaction and its influence on the LEMS curve is clearly present.

Ge detector is typically 10 to 20 ns. Therefore, the improvement of the peak to background ratio using the recoil-shadow configuration, i.e., separating target and host and shielding the detectors from the target, has been investigated. An experiment using the $^{nat}\text{Fe}(^{16}\text{O}, 2pn)^{69}\text{Ge}$ reaction with a beam energy of 65 MeV has been performed. The target thickness of 1.57 mg/cm² allowed all $^{69m}\text{Ge}[I^\pi = 9/2^+, \tau = 4.05(7) \mu\text{s}]$ recoils to reach the Pt host. Figure 3 shows that improvement of the peak to background ratio of the 398 keV $M2$ transition can go as high as a factor of 5 using the recoil-shadow geometry [24].

B. The influence of the $\vec{I} \cdot \vec{J}$ interaction on a LEMS curve

1. The influence on the anisotropy due to a combined magnetic dipole + $\vec{I} \cdot \vec{J}$ interaction

Several experiments using the $^{nat}\text{Fe}(^{16}\text{O}, 2pn)^{69}\text{Ge}$ reaction with a beam energy of 65 MeV have been performed at the CYCLONE cyclotron in Louvain-la-Neuve, Belgium. The target thickness of 1.57 mg/cm² is thin enough to re-

lease all recoils. The recoil energy is 15 MeV, but because of the energy loss in the target, the average energy with which the nuclei leave the target is $E_0 = 9$ MeV and the energy spread has been taken as $\sigma_E = 5$ MeV (TRIM [20] calculations). In a first experiment, the Ge isomers have been stopped in a 1.78 mg/cm² thick Ni host at a distance of 6 cm from the ^{nat}Fe target. A 50 μm thick Ta foil served as a beam stopper. The combination of a thin Ni foil + high-Z beam stopper has been chosen in order to decrease the reactions with the Ni. The Ni foil has been heated up to 450 °C to reach its paramagnetic phase. Since Ni is cubic, no EFG and thus no quadrupole interaction is present unless defects are trapped by the probe nuclei. An experiment applying the direct production in a thick Ni foil, using the $^{nat}\text{Ni}(^{12}\text{C}, 2pn)^{69}\text{Ge}$ reaction, proves that indeed no defects are created. This is shown by the analysis of the 398 keV $M2$ transition which does not show a change in the anisotropy as a function of B [Fig. 4(a)]. So if a change in the anisotropy is observed in the recoil-distance experiment, it is entirely due to the $\vec{I} \cdot \vec{J}$ interaction during the recoil time of the ^{69}Ge ions.

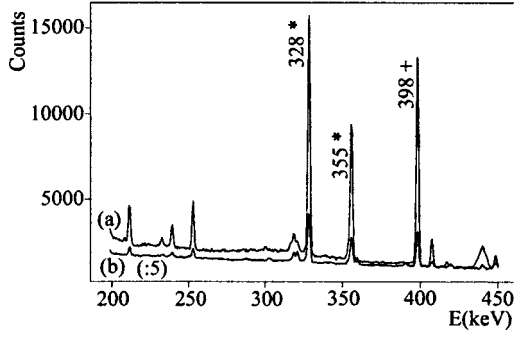


FIG. 3. Improvement of the peak to background ratio in a spectrum taken in a recoil-shadow configuration for the $^{nat}\text{Fe}(^{16}\text{O}, 2pn)^{69}\text{Ge}$ reaction. The peak originating from the $^{69}\text{Ge}(I=9/2)$ isomer, is marked with a plus, the Coulex peaks on Pt with an asterisk. For spectrum (b), no means to reduce the background radiation have been used. Spectrum (a) is taken in the recoil-shadow configuration. The number of counts of spectrum (b) is divided by a factor of 5 in order to make the background levels of spectrum (a) and (b) coincide.

Notice that the recoil time is only about 10 ns, which is much shorter than the isomeric lifetime of 4 μs .

The $\vec{I} \cdot \vec{J}$ decoupling curve for the $^{69}\text{Ge}(I=9/2)$ isomers with a recoil velocity $v_{\text{rec}} = 1.7\%c$ is shown in Fig. 4(b). The fit results in $\nu_{IJ}/\mu_B = 0.25_{-0.04}^{+0.06}$ GHz/ μ_B and $J = 2.7(2)$ where μ_B is the Bohr magneton. For comparison we mention that at a recoil velocity of $v_{\text{rec}} = 1.8\%c$ J takes values of $J = 3$ for the ^{54}Fe ions, $J = 3.5$ to 4.5 for the ^{107}Cd ions and $J = 5(1)$ for the ^{144}Gd ions [22]. An estimate of the atomic magnetic moment can be made using the relationship $\vec{\mu}_J = -g_J \vec{J} \mu_B / \hbar$ with the Landé g factor as a good approximation for the atomic gyromagnetic ratio g_J [27]. The Landé g factor is either 1 when the atomic intrinsic spin is $S=0$, or 2 when the atomic orbital angular momentum is $L=0$. The large total atomic angular momentum $J=2.7(2)$ indicates that a considerable amount of orbital angular momentum must be involved. Indeed the total atomic angular momentum averaged over the Hund ground states yields only 0.9 [11]. Therefore excited atomic states, where, e.g., several d electrons couple to high orbital momentum levels, must be present. This results in an approximate value of $g_J = 1$. This value is also confirmed by the general relationship

$$\frac{L+2S}{L+S} \geq g \geq \frac{L-2S+1}{L-S+1} \quad (20)$$

which is valid for $L \geq S$ [27]. Combining the fit results with the value obtained for g_J results in an atomic hyperfine field B_{hf} of 1080_{-175}^{+270} T. The difference with the results published in Ref. [25] is due to the fact that there the Landé g factor has been taken equal to 2.

2. The influence on the anisotropy due to the combined $\vec{I} \cdot \vec{J}$ + magnetic dipole + electric quadrupole interaction

In order to verify experimentally the combined LEMS + $\vec{I} \cdot \vec{J}$ interaction two experiments with the ^{69}Ge atomic nu-

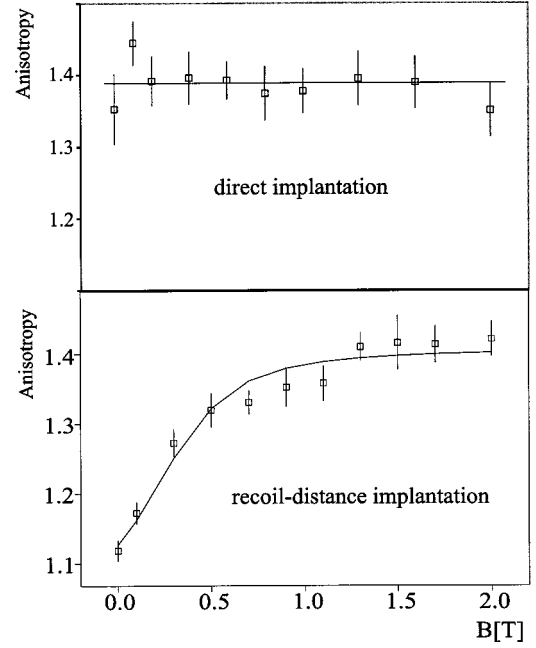


FIG. 4. (a) LEMS curve for the $^{69}\text{Ge}(I=9/2)$ isomer in Ni at 450 °C using a direct production in the Ni. No change of the spin orientation is measured, as a function of the externally applied magnetic field, proving that no defect-associated electric field gradients in the Ni are present. (b) $\vec{I} \cdot \vec{J}$ decoupling curve for the $^{69}\text{Ge}[I=9/2, \tau=4.05(7) \mu\text{s}]$ isomers recoiling out a ^{nat}Fe foil with a velocity of $1.7\%c$ and stopped in a Ni foil heated up to 450 °C after a 9 ns flight time. The ratio $\nu_{IJ}/\mu_B = 0.25_{-0.04}^{+0.06}$ GHz/ μ_B with $\nu_{IJ} = (\hbar/2\pi)a$ and $\mu_J = g_J J \mu_B$ corresponds for the approximate value of $g_J = 1$ with an atomic magnetic hyperfine field of 1080_{-175}^{+270} T.

clei recoiling into a Pt host have been performed. In a first experiment the ^{nat}Fe was evaporated on the Pt, while in a second one the Fe foil was placed at a recoil-distance of 6 cm. Pt is cubic but other experiments [26] have shown that defects are easily created in this host resulting in a defect-associated EFG. At zero recoil-distance a combined magnetic dipole + electric quadrupole interaction takes place. From the amplitude of the LEMS curve one can determine that 55(7)% of the Ge nuclei end up in a defect-associated site. 24(5)% of the Ge isomers are interacting with a smaller EFG [$\nu_{Q_1} = 6.4(1.5)$ MHz], while 31(5)% with a larger one [$\nu_{Q_2} = 18(2)$ MHz]. Figure 5 shows that the curve for a 6 cm recoil-distance has a larger amplitude which is caused by an extra lowering in the anisotropy due to the $\vec{I} \cdot \vec{J}$ interaction. In a first fit the $\vec{I} \cdot \vec{J}$ interaction was not taken into account in order to verify the influence of the $\vec{I} \cdot \vec{J}$ interaction on the quadrupole interaction frequencies. The same quadrupole frequencies, within the error bar, have been found (Table I). Only the fractions of the nuclei submitted to an EFG differ, since they are directly connected to the amplitude of the LEMS curve. In a second fit both the LEMS interaction and the $\vec{I} \cdot \vec{J}$ interaction have been taken into account. The $\vec{I} \cdot \vec{J}$ fit parameters have been fixed by the experiment with the Ni host and the quadrupole frequencies by the experiment with zero recoil distance. As a result also the fractions agree and

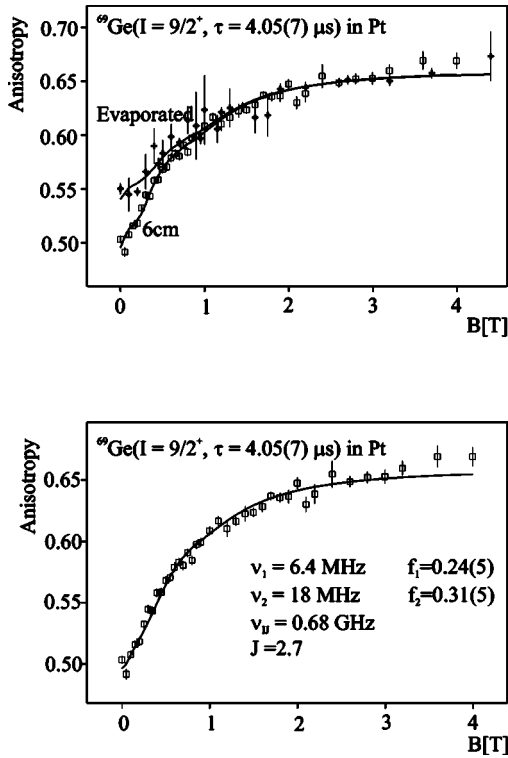


FIG. 5. (a) LEMS curves for the $^{69}\text{Ge}(I=9/2)$ isomer in Pt using zero and 6 cm recoil distances. No $\vec{I}\cdot\vec{J}$ interaction has been taken into account to fit the data. The fit results can be found in Table I. (b) Combined LEMS + $\vec{I}\cdot\vec{J}$ fit for the 6 cm recoil distance.

the theoretical curve is in better agreement with the experimental data. The improvement in χ^2 is 10%.

IV. CONCLUSION

Since the LEMS technique is applied to measure quadrupole moments of high-spin isomers, the atomic spin J is usually small compared to the nuclear spin I . Therefore the loss

TABLE I. Fit results for the $^{69}\text{Ge}(I=9/2)$ isomer in Pt with a zero and a 6 cm recoil distance. For a zero recoil distance only the pure LEMS interaction takes place. For a 6 cm recoil distance also the $\vec{I}\cdot\vec{J}$ interaction is present, which has been taken into account in (b), but not in (a).

d	ν_{Q_1} (MHz)	ν_{Q_2} (MHz)	f_1	f_2	ν_{IJ} (GHz)	J
0	6.4(1.5)	18(2)	0.24(5)	0.31(5)		
6 cm (a)	5.0(0.8)	17(4)	0.50(8)	0.40(5)	not in fit	not in fit
6 cm (b)	6.4	18	0.24(5)	0.31(5)	0.68	2.7

of orientation due to the $\vec{I}\cdot\vec{J}$ interaction is small compared to the loss of orientation due to the quadrupole interaction, even when large magnetic hyperfine fields created by the atomic electrons are present at the position of the nucleus. Indeed it is proven by the experiments on Ge(Pt) and the simulations that the influence of the $\vec{I}\cdot\vec{J}$ coupling on the fit results for the quadrupole frequencies, derived from a LEMS curve, is negligible. Even when this is not the case, a LEMS measurement in combination with the recoil-shadow geometry can be applied, because a combined LEMS + $\vec{I}\cdot\vec{J}$ fit produces the correct quadrupole frequencies. Moreover the $\vec{I}\cdot\vec{J}$ fit parameters (the atomic spin J and the hyperfine field B_{hf}) can be determined in an additional experiment where the nuclei of interest recoil substitutionally into a cubic host.

ACKNOWLEDGMENTS

The authors are very grateful to G.F. Hoy for his careful reading of the manuscript. N.C. and S.T. acknowledge the Flemish Institute for the Promotion of Scientific and Technological Research in the Industry (IWT) for providing grants. This work is partially financed by the IUAP project No. p4-07, with a grant for G.G. G.N. acknowledges support of the Flemish Science Foundation (FWO-Vlaanderen).

- [1] G. Scheveneels, F. Hardeman, G. Neyens, and R. Coussement, *Hyperfine Interact.* **52**, 257 (1989).
- [2] G. Neyens, R. Nouwen, and R. Coussement, *Nucl. Instrum. Methods Phys. Res. A* **340**, 555 (1994).
- [3] G. Neyens, N. Coulier, S. Ternier, K. Vyvey, S. Michiels, R. Coussement, D.L. Balabanski, J.M. Casandijan, M. Chartier, D. Cortina-Gil, M. Lewitowicz, W. Mittig, A.N. Ostrowski, P. Roussel-Chomaz, N. Alamanos, and A. Lépine-Szily, *Phys. Lett. B* **393**, 36 (1997).
- [4] G. Neyens, N. Coulier, S. Teughels, G. Georgiev, B.A. Brown, W.F. Rogers, D.L. Balabanski, R. Coussement, A. Lépine-Szily, M. Lewitowicz, W. Mittig, F. de Oliveira Santos, P. Roussel-Chomaz, S. Ternier, K. Vyvey, and D. Cortina-Gil, *Phys. Rev. Lett.* **82**, 497 (1999).
- [5] N. Coulier, G. Neyens, S. Teughels, D.L. Balabanski, R. Coussement, G. Georgiev, S. Ternier, and K. Vyvey, *Phys. Rev. C* **59**, 1935 (1999).
- [6] F. Hardeman, G. Scheveneels, G. Neyens, R. Nouwen, G. S'heeren, M. Van den Bergh, and R. Coussement, *Phys. Rev. C* **43**, 130 (1991).
- [7] F. Hardeman, G. Scheveneels, G. Neyens, R. Nouwen, G. S'heeren, M. Van den Bergh, and R. Coussement, *Phys. Rev. C* **43**, 514 (1991).
- [8] G. Neyens, R. Nouwen, G. S'heeren, M. Van Den Bergh, and R. Coussement, *Nucl. Phys.* **A555**, 629 (1993).
- [9] K. Vyvey, G. Neyens, D.L. Balabanski, S. Ternier, N. Coulier, S. Teughels, G. Georgiev, R. Wyckmans, R. Coussement, M. Mineva, P.M. Walker, A.P. Byrne, G.D. Dracoulis, and P. Blaha, *J. Phys. G* **25**, 767 (1999).
- [10] G. Scheveneels, F. Hardeman, G. Neyens, and R. Coussement, *Hyperfine Interact.* **52**, 179 (1989).
- [11] K. Vyvey, G. Neyens, S. Cottenier, N. Coulier, R. Coussement, G. Georgiev, S. Ternier, S. Teughels, A. Lépine-Szily, and D.L. Balabanski (unpublished).

- [12] R.M. Steffen and K. Alder, in *The Electromagnetic Interaction in Nuclear Spectroscopy* (North-Holland, Amsterdam, 1975), p. 505.
- [13] G. Goldring, in *Heavy Ion Collisions*, edited by R. Bock (North-Holland, Amsterdam, 1982), p. 483.
- [14] C. Broude, M.B. Goldberg, G. Goldring, M. Hass, M. J. Renan, B. Sharon, Z. Shkedi, and D.F.H. Start, Nucl. Phys. **A215**, 617 (1973).
- [15] A. Little, H.C. Jain, S. M. Lazarus, T.K. Saylor, B.B. Triplett, and S.S. Hanna, Hyperfine Interact. **8**, 3 (1980).
- [16] E. Matthias, W. Schneider, and R.M. Steffen, Phys. Rev. **125**, 261 (1962).
- [17] U. Fano and G. Racah, *Irreducible Tensorial Sets* (Academic, New York, 1959).
- [18] C. Cohen-Tannoudji, J. Dupont-Roc, and G. Grynberg, in *Processus d'Interaction Entre Photons et Atoms* (Inter Editions, Paris, 1988), p. 250.
- [19] R.J. Elliot and K.W.H. Stevens, Proc. R. Soc. London **218**, 553 (1953).
- [20] J.F. Ziegler and J.P. Biersack, *TRIM, TRansport of Ions in Matter* (Pergamon, New York, 1985).
- [21] H.J. Jansch and D. Fick, Z. Phys. D: At., Mol. Clusters **9**, 117 (1988).
- [22] E. Dafni, J. Bendahan, C. Broude, G. Goldring, M. Hass, E. Naim, M.H. Rafailovich, C. Chasman, O.C. Kistner, and S. Vajda, Nucl. Phys. **A443**, 135 (1985).
- [23] H.R. Andrews, R.L. Graham, J.S. Geiger, J.R. Beene, O. Häusser, D. Ward, and D. Horn, Hyperfine Interact. **4**, 110 (1978).
- [24] K. Vyvey, G. Neyens, S. Ternier, N. Coulier, S. Michiels, R. Coussement, D.L. Balabanski, and A. Lépine-Szily, Acta Phys. Pol. B **28**, 329 (1997).
- [25] K. Vyvey, G. Neyens, D.L. Balabanski, S. Ternier, N. Coulier, S. Teughels, G. Georgiev, and R. Coussement, in *Proceedings on the International Conference on "The Nucleus: New Physics for the New Millennium"* Strand, South-Africa, 1999 (unpublished), p. 457.
- [26] S. Ternier, G. Neyens, K. Vyvey, J. Odeurs, N. Coulier, S. Michiels, R. Coussement, D.L. Balabanski, and R. Kulkarni, Nucl. Instrum. Methods Phys. Res. B **140**, 235 (1998).
- [27] I.I. Sobelman, *Atomic Spectra and Radiative Transitions* (Springer-Verlag, Berlin, 1979).